Available online at www.sciencedirect.com

SciVerse ScienceDirect

Ceramics International 38 (2012) 1975–1980

CERAMICS INTERNATIONAL

www.elsevier.com/locate/ceramint

A study on the photoluminescence properties of electrospray deposited amorphous and crystalline nanostructured ZnO thin films

A. Hosseinmardi, N. Shojaee *, M. Keyanpour-Rad, T. Ebadzadeh

Materials and Energy Research Center (MERC), P.O. Box 14155-4777, Alborz, Iran

Received 31 July 2011; received in revised form 4 October 2011; accepted 13 October 2011
Available online 18 October 2011

Abstract

Transparent amorphous and crystalline nanostructured zinc oxide (ZnO) thin films were prepared by electrospray deposition technique on a glass substrate at 250 °C using zinc nitrate and ammonia as the precursors. The structural morphology and optical properties of the thin films were evaluated and also the effect of formation rate of basic generating species on the morphology of the thin films was discussed. Optical studies indicated that all of the thin films have a near band edge emission at 374 nm and a band gap of 3.32 eV. In addition, the films have an emission at 393 nm corresponding to ultra violet (UV) transmittance. However, the amorphous thin films have oxygen trap peak at 430 nm and two green transmittance peaks at 485 nm and 530 nm which are absent in the 0.1 molar nanostructured sample. The crystallite size of the thin films which calculated from XRD patterns via Debye–Scherrer's formula was around 30 nm.

Keywords: D. ZnO; Thin film; Electrospray deposition; Optical property

1. Introduction

Zinc oxide (ZnO), a direct wide band gap (3.4 eV) n-type semiconductor compound, has a stable wurtzite structure. This oxide has attracted intensive research efforts for its unique properties and versatile applications in piezoelectric devices, ultraviolet light emitters, transparent electronics, chemical sensors, electronics and, etc. [1–5].

ZnO forms many morphologies and structures such as single crystals [6], nanocrystals [7], nanorods [8], thick and thin films [9]. Most of the researches are centered on the synthesis of single crystal ZnO thin films, while amorphous semiconductors, which relax the k-selection rules for the optical transitions, have some advantages that can be used instead, decreasing the expense of preparing large single crystal sheets [10]. Its thin film has a strong piezoelectricity and photoelectric effect and is known to have advantageous characteristics in many areas in comparison to conventional compounds, such as GaN. In addition, ZnO thin film has excellent transmittance in the infrared and visible light regions, electrical conductivity and durability to plasma while cost of its raw material is also economical. Therefore, the application range of ZnO thin films is very wide. For example, it is used as transparent electrodes, photocatalysts, energy saving coating materials for window glasses, acousto-optic devices, ferroelectric memories, solar cells and reduction gas detection sensors [11–13].

Techniques for growing ZnO thin films include various coating methods such as chemical vapor deposition [14], sol–gel [15], plasma assisted molecular beam epitaxy [16], electrostatic spray deposition [17], microwave-assisted hydrothermal [18], pulse laser deposition [19], atomic layer deposition [20] and magnetron sputtering [21]. Most of these methods are accompanied by some restrictions like using expensive and sophisticated instruments, high vacuum and temperatures. The hydrothermal methods that use water as media, also suffer from long reaction times [22,23]. Electrostatic deposition methods of making thin films have many advantages, such as simple setup, low cost, non toxic precursors, easy control of morphology and stoichiometry, attaining nano structures and high deposition efficiency, over some conventional deposition techniques [24,25]. Also preparation parameters create significant changes in the crystal

* Corresponding author. Tel.: +98 912 2630860; fax: +98 21 66017496.
E-mail addresses: arhm1364@gmail.com (A. Hosseinmardi), n_shojaee@merc.ac.ir, nash1390@gmail.com (N. Shojaee), m_kianpourrad@yahoo.com (M. Keyanpour-Rad), ebadzadehtouradj@yahoo.co.uk (T. Ebadzadeh).

0272-8842/$36.00
doi:10.1016/j.ceramint.2011.10.031

grain shape, size and orientation, intrinsic stress, defect densities, electrical and optical properties, chemical stoichiometry and surface morphologies [26,25].

In this study, the electrospray deposition of both amorphous and crystalline ZnO structures on glass substrates was reported using easy available and cheap precursors. The aim of this work was to investigate the effect of zinc nitrate and some alkali precursors in formation of ZnO thin film via electrospraying method. The structural and photoluminescence properties of the transparent layers were also studied. On the basis of Fourier Transform Infrared (FTIR) analysis the use of a faster generating basic material, like ammonia, were suggested instead of hexamethylene tetramine.

2. Materials and methods

2.1. Reagents

All chemicals (MERCK Chemical Company) used in this work were of analytical reagent grades and used with no further purification. Ordinary glass plates were used as substrate and washed ultrasonically in alcohol, acetone and double distilled water, respectively, and finally dried at room temperature.

2.2. Electrospray deposition in aqueous solution

A homogeneous solution was prepared by dissolving zinc nitrate hexahydrate [$Zn(NO_3)_2{\cdot}6H_2O$] and hexamethylene tetramine, HMT [$(CH_2)_6N_4$] or ammonia (25%) in distilled water. 3–4 drops of nitric acid (65%) were added to some of the above solutions in order to prevent premature precipitation of the ions prior to the electrospraying step. The molar ratio of the starting materials was kept 1:1 in the final solutions.

Deposition of ZnO thin films was performed using an electrostatic spray deposition set up with horizontal configuration having a controllable heater for maintaining the substrate temperature at 250 °C [27]. The horizontal electrospraying setup was equipped with a 50 ml syringe and a stainless steel needle (inner diameter of 0.495 mm and length of 0.5 in.) on the syringe pump (Top 5300) to control the feed rate (1 ml/h). The distance between syringe and the collector was set at 15 cm. A high voltage (12 kV) was applied via a high voltage DC power supply (Glassman High Voltage Inc.) and the process was carried out at room temperature. Fig. 1 shows the schematic of electrospray setup. Different samples with various conditions were made to find out their effects on the morphology of the thin films (Table 1).

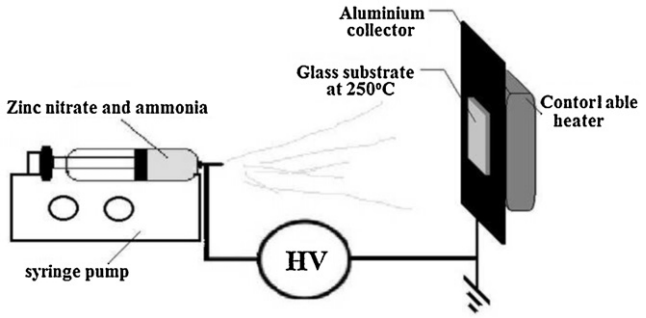

Fig. 1. Schematic of electrospray setup.

2.3. Characterizations

FTIR analysis was carried out on a Perkin-Elmer spectrometer, spectrum 400, in the form of KBr pellet. Powder X-ray Diffraction (XRD) analysis was performed on Unisantis-XMD 300 diffractometer with nickel-filtered Cu K_α radiation ($\lambda = 1.542$ Å). The morphology of the thin films was characterized by optical microscopy (Olympus, BX61), Scanning Electron Microscopy (SEM, Phillips, XLC) and Field Emission Scanning Electron Microscopy (FESEM, Hitachi, HIT 4160). The photoluminescence spectroscopy (PL) was done at room temperature on a Perkin-Elmer LS-5 spectrometer, using xenon lamp with a wavelength of 325 nm as the excitation source.

3. Results and discussion

Fig. 2 shows the FTIR spectrum of all deposited films. In sample specified as ZO1, the band centered at about 3500 cm^{-1} shows the characteristic of OH stretching vibration of absorbed water. The most intense band at 1384.19 cm^{-1} and also the sharp band at 825.43 cm^{-1} are both attributed to inorganic ionic nitrate compounds [28]. In this spectrum, the sharp band at 1668.71 cm^{-1} is the characteristic of carbonyl stretching vibration of an aldehyde, mostly resembling the trimeric form of formaldehyde, which result from decomposition of HMT in water [29]. Therefore, the gummy, non-transparent film obtained from sample ZO1 could be characterized as a mixture of starting inorganic zinc compound and trimeric formaldehyde. It is already known that an advantage of using HMT in hydrothermal synthesize of ZnO thin films is the slow rate of decomposition of this amine in water to form formaldehyde and ammonia which subsequently reacts with Zn^{2+} ions to form $Zn(OH)_2$ which finally converts to ZnO [30]. But it seems that the slow rate of formation of ammonia from decomposition of HMT is a major drawback in electrospray method for the preparation of ZnO thin films. Therefore, ammonia was directly used as the base generating species, because it furnishes faster and creates more OH^- in the solution and therefore ZO1 was eliminated for further analysis.

Table 1
Ingredients and concentration conditions of the precursors.

Sample	Zinc nitrate	Ammonia	HMT	Concentration (molar)
ZO1	×		×	0.5
ZO2[a]	×	×		0.5
ZO3	×	×		0.5
ZO4[a]	×	×		0.1
ZO5	×	×		0.1

[a] With addition of nitric acid.

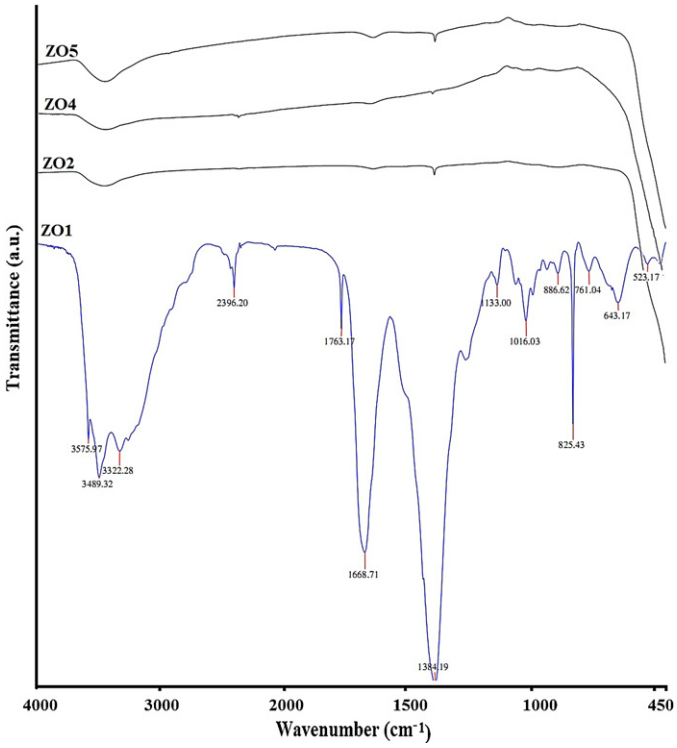

Fig. 2. FTIR spectra of samples ZO1, ZO2, ZO4 and ZO5.

In sample ZO3 early precipitation was occurred and resulted in a segregated solution in the syringe that could not be electrosprayed. Therefore some droplets of nitric acid were added to the solution and the sample ZO3 was eliminated. On the other hand, the spectra corresponding to ZO2, ZO4 and ZO5 samples were pure and similar to each other. In contrast to sample ZO1, these samples did not have organic peaks and showed bands at 3200–3500 cm^{-1} and 1640 cm^{-1} corresponding to the stretching and bending vibrations of hydroxyl groups on ZnO thin film surface, respectively. According to the results obtained by Begum, Sugunan, Rasouli and Padmanabhan results [31–34], it can be concluded that ZO2, ZO4 and ZO5 samples are formed as pure substances. The stepwise reactions taking place in the process of formation of the thin films are outlined below:

$$NH_3 + H_2O \leftrightarrow NH_4^+ + OH^- \quad (1)$$

$$Zn(NO_3)_2{\cdot}6H_2O + H_2O \leftrightarrow Zn^{2+} + 2NO_3^- + 7H_2O \quad (2)$$

$$Zn^{2+} + 2OH^- \rightarrow Zn(OH)_2 \quad (3)$$

$$Zn(OH)_2 \rightarrow ZnO + H_2O \quad (4)$$

In the above process, a white precipitate was immediately formed after addition of ammonia to zinc nitrate hexahydrate. The solution was turned clear by addition of a few drops of nitric acid (65%) and therefore became suitable for use in the electro spray deposition method. The crystallites were formed as an effect of solvent evaporation from the droplet on its flight toward the substrate.

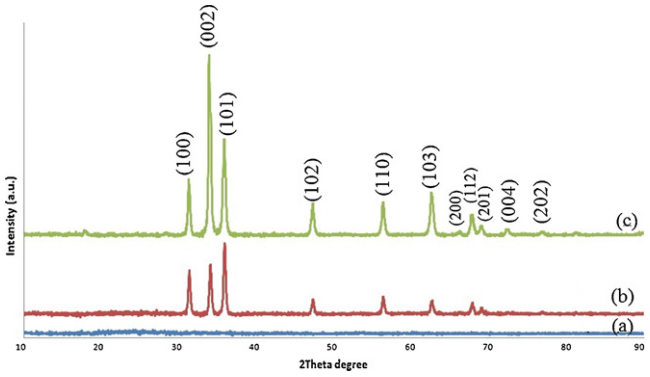

Fig. 3. X-ray diffraction patterns of deposited ZnO thin films: (a) ZO2, (b) ZO5 and (c) ZO4.

Fig. 3 shows the XRD spectra of deposited ZnO thin films. In the case of ZO4, an amorphous thin film was observed, while ZO2 and ZO5 samples were formed in high degree of crystallinity with wurtzite hexagonal polycrystalline structure (referred to JCPDS cards no. 36-1451, $a = 0.325$ nm, $c = 0.521$ nm). No diffraction peaks from impurity phases were detected in any samples within the limit of our XRD measurements. The crystallite size was calculated using Debye–Scherrer equation:

$$L = \frac{0.94\,\lambda}{\beta \cos\theta}$$

where λ, θ and β are X-ray wavelength, the Bragg's diffraction angle and the full width at half maxima (FWHM) of the peak corresponding to the "θ" value, respectively [35]. The crystallite size was found to be from 32 to 28 nm at an angle 2θ from 34.2° to 36.2° in cases of ZO2 and ZO5, respectively. The degree of growth orientation was calculated via the following equation, using relative texture coefficient [36]:

$$TC_{002} = \frac{I_{002}/I^0_{002}}{(I_{002}/I^0_{002}) + (I_{101}/I^0_{101})}$$

where $TC_{0\,0\,2}$ is the relative texture coefficient of diffraction peaks (0 0 2) over (1 0 1), $I_{0\,0\,2}$ and $I_{1\,0\,1}$ are the measured diffraction intensities corresponding to (0 0 2) and (1 0 1) planes, respectively. I^0_{002} and I^0_{101} are the values of standard diffraction intensities measured from randomly oriented powder samples. For materials with random crystallographic orientation, $TC_{0\,0\,2}$ equals to 0.5 [36]. The values of the $TC_{0\,0\,2}$ in our samples are 0.83 and 0.61 for ZO2 and ZO5, respectively, which indicate that ZO2 has an obvious c-orientation, while ZO5 has a nearly random orientation.

For sample ZO4, some droplets of the acid were added to the solution in order to prevent the early precipitation. It seems that in low concentration, the acid has postponed the reaction to take place, resulting in very fine particles which were not detectable for the XRD instrument. Unlike traditional methods which need temperature change (even up to 800 °C) to reach amorphous structures, in this method amorphous ZnO layer is synthesized just using nitric acid as a stabilizer and pH modifier.

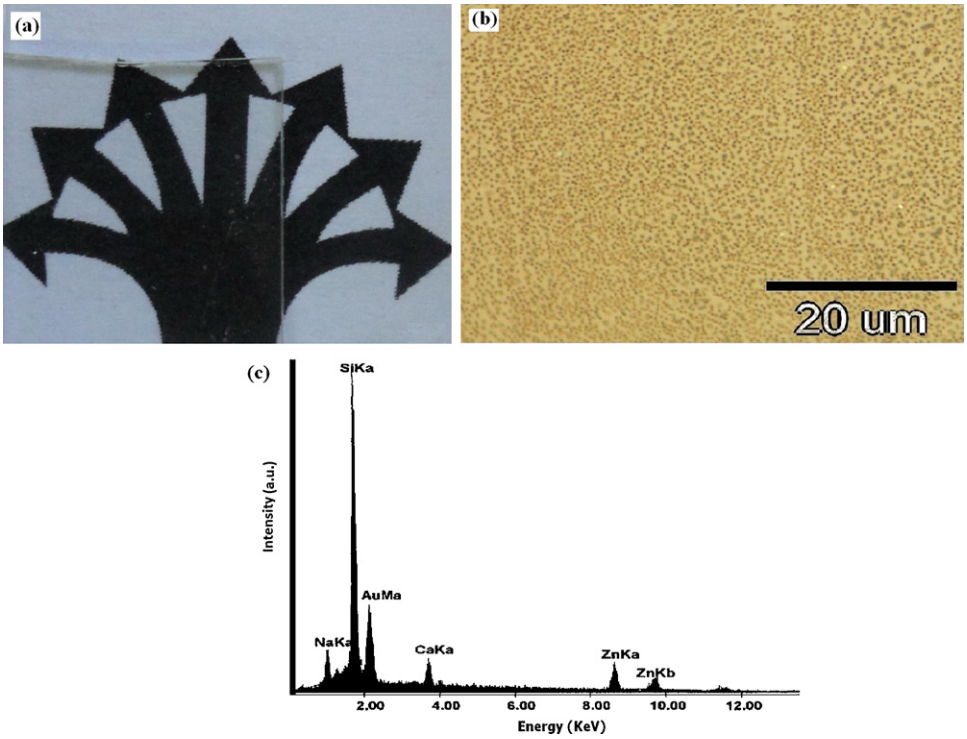

Fig. 4. (a) A 20 mm × 15 mm transparent thin film (b) optical microscopy and (c) EDS of ZO5.

Fig. 4(a) shows a ZnO coated glass on a patterned sheet in order to prove its transparency. Fig. 4(b) illustrates the optical microscopy of the sample. As this figure shows, the droplets were smoothly spread on the surface and as a result, a homogenized layer was deposited on the glass substrate. The Si, Na and Ca peaks in EDS spectra of ZO5 (Fig. 4(c)) were related to the glass substrate and Au peak was related to the gold coating in the process of SEM sample preparation. Therefore, it can be concluded that the coated layer should be the pure ZnO. Since the results of all samples (ZO2, ZO4 and ZO5) were the same, therefore only ZO5 was picked as a candidate in Fig. 4.

Fig. 5(a)–(c) shows the SEM images of ZO2, ZO4 and ZO5 samples. In electrospray process a high voltage motivates solution spray. The solvent vaporizes during the spray process

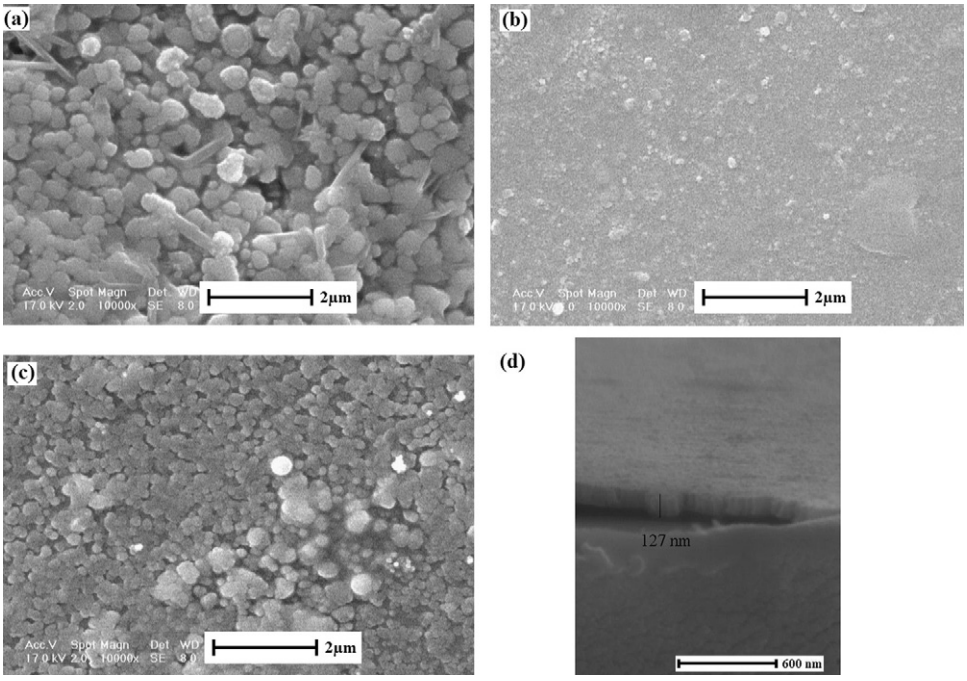

Fig. 5. SEM images of: (a) ZO2, (b) ZO4, (c) ZO5 and (d) cross section of ZO4.

and as the positive charge accumulate and repulse each other, the droplets divided in to several small drops and nano sized crystals reach the collector. Crystal growth behavior of ZnO nanostructures depends on the varied coagulation patterns of ZnO nuclei in preferred axes, affecting the shape, size and assembling pattern of the building blocks. The preferred axes of coagulation are due to the capping of cation-complexes and anions onto the differently charged crystal planes of ZnO nuclei. The resultant morphology is largely dependent on the amount of capping which in turn is a function of the stability of the cation-complexes and the anion's in the solution and also the amount of ZnO nuclei in the solution [37]. The XRD results demonstrate samples have different crystallographic orientations, but it seems that there is not enough time for the particles to build different morphologies and therefore, a thin film is formed from these particles. The quality of thin films formed on the substrates strongly depends on the size of particles or droplets forming the layer and their monodispersity. It could be demonstrated from these figures that lower precursor concentrations should be used to obtain more uniform coating with a lower roughness which are compatible with Jaworek findings [25]. Fig. 5(d) illustrates a FESEM cross sectional image of ZO4. The thickness of deposited layer was measured to be 127 nm.

To study the affect of variables on photoluminescence properties of ZnO thin films, PL measurements were carried out at room temperature under the excitation of 325 nm, which is shown in Fig. 6. The peak at around 374 nm corresponds to near band-edge emission of ZnO nano particles, and consequently the band gap calculated using the Plank's equation was 3.32 eV. The PL spectrum shows a peak at 393 nm which is due to ultraviolet emission of ZnO. The UV emission is attributed to the near band edge emission of ZnO which is due to decay of excitons [38]. The weak emission peaks at about 430 nm in ZO2 and ZO4 corresponded to the existence of oxygen depletion interface traps in the ZnO_x thin film which is compatible with Jin et al. findings [19]. In addition, there are two green light luminescence peaks at about 485 and 530 nm in ZO4 which are in agreement with the results found by Vanheusden et al. [39]. These peaks are due to deep-level or trap-state emission, corresponding to the ionized oxygen vacancies in the ZnO thin films. According to the energy band gap of oxygen vacancy, the peak at approximately 485 nm results from radiative recombination of a hole related to the zinc vacancy with an electron occupying the low oxygen vacancy energy bands. The peak at about 530 nm is due to the radiative recombination of a photogenerated hole in the valence band with an electron occupying the deep oxygen vacancy energy band [36]. The intensity of peaks is weak because of low density of oxygen vacancies in the ZnO thin films. The blue shift and extra peaks observed in UV emission of ZO4 can be attributed to the amorphous structure and structural deficiencies. The results of transmittance are expected to depend on several factors, such as oxygen deficiencies, surface roughness and impurity centers [17]. It can be assumed that the lower transmittance of ZO2 is mainly due to the surface roughness of the film. In general, the electrosprayed zinc oxide thin films exhibits n-type behaviors due to the compensation effect of shallow donors induced by oxygen vacancies, zinc interstitials, and antisite defects [40].

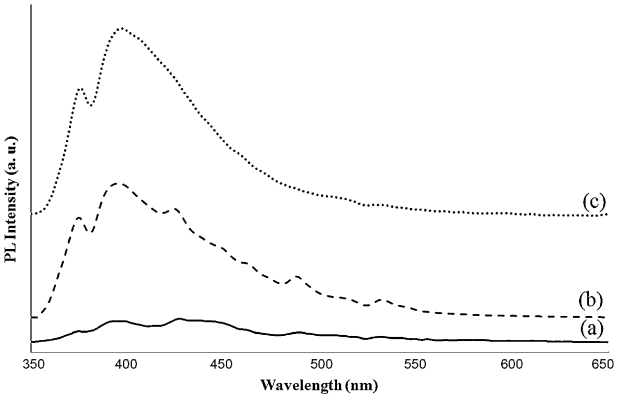

Fig. 6. Room temperature photoluminescence spectrum of samples: (a) ZO2, (b) ZO4 and (c) ZO5.

4. Conclusions

Both crystallized (28–32 nm) and amorphous transparent ZnO thin films were grown on glass substrates by simple electrospray deposition method, using cheap starting materials and low operating temperatures. FTIR analysis of the gummy product obtained from the reaction of zinc nitrate and HMT suggested that the product obtained as a mixture of mostly starting nitrate and also some trimeric formaldehydes. Therefore, it was decided that HMT, which slowly generates basic species into aqueous solution, was not a proper candidate to be used in electrospray method and therefore it was replaced by ammonia which generates faster basic species in the solution. It was also found that the addition of small amounts of dilute HNO_3 could have direct effect on the morphology of the thin films. The band gap of the deposited transparent thin films at this temperature reached the value of 3.32 eV.

Acknowledgement

We are thankful to Materials and Energy Research Center (MERC) for partial financial support of this work.

References

[1] F.S. Chien, C.R. Wang, Y.L. Chan, S.L. Lin, M.H. Chen, R.J. Wu, Fast response ozone sensor with ZnO nanorods grown by chemical vapor deposition, Sens. Actuators B 144 (2010) 120–125.
[2] W.S. Han, Y.Y. Kim, B.H. Kong, H.K. Cho, Ultraviolet light emitting diode with n-ZnO:Ga/i-ZnO/p-GaN:Mg heterojunction, Thin Solid Films 517 (2009) 5106–5109.
[3] S. Singh, P. Thiyagarajan, K.M. Kant, D. Anita, S. Thirupathiah, N. Rama, B. Tiwari, M. Kottaisamy, M.S.R. Rao, Structure, microstructure and physical properties of ZnO based materials in various forms: bulk, thin film and nano, J. Phys. D: Appl. Phys. 40 (2007) 6312–6327.
[4] I.T. Tang, H.J. Chen, W.C. Hwang, Y.C. Wang, M.P. Houng, Y.H. Wang, Applications of piezoelectric ZnO film deposited on diamond-like carbon coated onto Si substrate under fabricated diamond SAW filter, J. Cryst. Growth 262 (2004) 461–466.

[5] R. Vinodkumar, K.J. Leth, P.R. Arunkumar, R.R. Krishnan, N.V. Pillai, V.P.M. Pillai, R. Philip, Effect of cadmium oxide incorporation on the microstructural and optical properties of pulsed laser deposited nanostructured zinc oxide thin films, Mater. Chem. Phys. 121 (2010) 406–413.
[6] S.H. Hong, M. Mikami, K. Mimura, M. Uchikoshi, A. Yasuo, S. Abe, K. Masumoto, M. Isshiki, Growth of high quality ZnO single crystals by seeded CVT using the newly designed ampoule, J. Cryst. Growth 311 (2009) 3609–3612.
[7] S. Yamamoto, H. Yano, T. Mishina, J. Nakahara, Decay dynamics of ultraviolet photoluminescence in ZnO nanocrystals, J. Lumin. 126 (2007) 257–262.
[8] J. Zhao, D. Wu, J. Zhi, A novel tyrosinase biosensor based on biofunctional ZnO nanorod microarrays on the nanocrystalline diamond electrode for detection of phenolic compounds, Bioelectrochemistry 75 (2009) 44–49.
[9] S. O'Brien, M.G. Nolan, M. Copuroglu, J.A. Hamilton, I. Povey, E. Fortunato, Zinc oxide thin films: characterization and potential applications, Thin Solid Films 518 (2010) 4515–4519.
[10] J.M. Khoshman, M.E. Kordesch, Optical constants and band edge of amorphous zinc oxide thin films, Thin Solid Films 515 (2007) 7393–7399.
[11] F. Sette, S. Pearton, D. Norton, K. Ip, Y.W. Heo, T. Steiner, Local structure of S impurities in GaAs, Prog. Mater. Sci. 50 (2005) 293–340.
[12] M. Krunks, A. Katerski, T. Dedova, I.O. Acik, A. Mere, Nanostructured solar cell based on spray pyrolysis deposited ZnO nanorod array, Sol. Energy Mater. Sol. Cells 92 (2008) 1016–1019.
[13] N.T. Salim, K. Aw, B. Wright, ZnO as dielectric for optically transparent non-volatile memory, Thin Solid Films 518 (2009) 362–365.
[14] G.Z. Wang, Y. Wang, M.Y. Yau, C.Y. To, C.J. Deng, D.H.L. Ng, Synthesis of ZnO hexagonal columnar pins by chemical vapor deposition, Mater. Lett. 59 (2005) 3870–3875.
[15] T. Ivanova, A. Harizanova, T. Koutzarova, B. Vertruyen, Study of ZnO sol–gel films: effect of annealing, Mater. Lett. 64 (2010) 1147–1149.
[16] S.M. Yang, S.K. Han, J.W. Lee, J.-H. Kim, S.K. Hong, J.Y. Lee, J.H. Song, S.I. Hong, J.S. Park, T. Yao, Microstructural investigation of ZnO films grown on (1 1 1) Si substrates by plasma-assisted molecular beam epitaxy, J. Cryst. Growth 312 (2010) 1557–1562.
[17] K.S. Hwang, J.H. Jeong, Y.S. Jeon, K.O. Jeon, B.H. Kim, Electrostatic spray deposited ZnO thin films, Ceram. Int. 33 (2007) 505–507.
[18] N. Shojaee, T. Ebadzadeh, A. Aghaei, Effect of concentration and heating conditions on microwave-assisted hydrothermal synthesis of ZnO nanorods, Mater. Charact. 61 (2010) 1418–1423.
[19] B.J. Jin, S. Im, S.Y. Lee, Violet UV luminescence emitted from ZnO thin films grown on sapphire by pulsed laser deposition, Thin Solid Films 366 (2000) 107–110.
[20] M. Godlewski, E. Guziewicz, T. Krajewski, A. Wachnicka, K. Kopalko, A. Sarem, B. Dalat, ZnO layers grown by Atomic Layer Deposition: a new material for transparent conductive oxide, Thin Solid Films 518 (2009) 1145–1148.
[21] W. Gao, Z. Li, ZnO thin films produced by magnetron sputtering, Ceram. Int. 30 (2004) 1155–1159.
[22] L. Vayssieres, Growth of arrayed nanorods and nanowires of ZnO from aqueous solutions, Adv. Mater. 15 (2003) 464–466.
[23] S.H. Jung, S.H. Jeong, Selective-area growth of ZnO nanorod arrays via a sonochemical route, Mater. Lett. 62 (2008) 3673–3675.
[24] A. Jaworek, Electrospray droplet sources for thin film deposition, J. Mater. Sci. 42 (2007) 266–297.
[25] A. Jaworek, A.T. Sobczyk, Electrospraying route to nanotechnology: an overview, J. Electrostat. 66 (2008) 197–219.
[26] V. Tvarozek, I. Novotny, P. Sutta, S. Flickyngerova, K. Schtereva, E. Vavrinsky, Influence of sputtering parameters on crystalline structure of ZnO thin films, Thin Solid Films 515 (2007) 8756–8760.
[27] A. Bazargan, M.A. Fateminia, M.E. Ganji, M.A. Bahrevar, Electrospinning preparation and characterization of cadmium oxide nanofibers, Chem. Eng. J. 155 (2009) 523–527.
[28] R. Wahab, S.G. Ansari, Y.S. Kim, M.A. Dar, H.-S. Shin, Synthesis and characterization of hydrozincite and its conversion into zinc oxide nanoparticles, J. Alloys Compd. 461 (2008) 66–71.
[29] R. Song, Y. Liu, L. He, Synthesis and characterization of mercaptoacetic acid-modified ZnO nanoparticles, Solid State Sci. 10 (2008) 1563–1567.
[30] l. vayssieres, An aqueous solution approach to advanced metal oxide arrays on substrates, Appl. Phys. A 89 (2007) 1–8.
[31] P.M.S. Begum, K.M. Yusuff, R. Joseph, Preparation and use of nano zinc oxide in neoprene rubber, Int. J. Polym. Mater. 57 (2008) 1083–1094.
[32] A. Sugunan, H.C. Warad, M. Boman, J. Dutta, Zinc oxide nanowires in chemical bath on seeded substrates: role of hexamine, J. Sol–Gel Sci. Technol. 39 (2006) 49–56.
[33] S. Rasouli, S. Saket, One step rapid synthesis of nano-crystalline ZnO by microwave-assisted solution combustion method, Prog. Color Colorants Coat. 3 (2010) 19–25.
[34] S.C. Padmanabhan, D. Ledwith, S.C. Pillai, D.E. McCormack, J.M. Kelly, Microwave-assisted synthesis of ZnO micro-javelins, J. Mater. Chem. 19 (2009) 9250–9259.
[35] B.D. Cullity, Elements of X-ray Diffractions, Addison-Wesley, MA, 1978
[36] F. Li, Z. Li, F.J. Jin, Structural and luminescent properties of ZnO nanorods prepared from aqueous solution, Mater. Lett. 61 (2007) 1876–1880.
[37] V. Pachauri, K. Kern, K. Balasubramanian, Template free self-assembly of hierarchical ZnO structures from nanoscale building blocks, Chem. Phys. Lett. 498 (2010) 317–322.
[38] D.H. Zhang, Q.P. Wang, Z.Y. Xue, Photoluminescence of ZnO films excited with light of different wavelength, Appl. Surf. Sci. 207 (2003) 20–25.
[39] K. Vanheusden, W.L. Warren, C.H. Ceager, D.R. Tallant, J.A. Voigt, B.E. Gnade, Mechanisms behind green photoluminescence in ZnO phosphor powders, J. Appl. Phys. 79 (1996) 7983–7990.
[40] Y.S. Chiu, C.Y. Tseng, C.T. Lee, Nanostructured EGFET pH sensors with surface-passivated ZnO thin-film and nanorod array, IEEE Sens. J. (2011), 1-1.